Catalysis Science & Technology

Recent Advances of Reducible Metal Oxide Catalysts in C1 Reactions

Journal:	*Catalysis Science & Technology*
Manuscript ID	CY-MRV-08-2022-001531.R2
Article Type:	Minireview
Date Submitted by the Author:	04-Nov-2022
Complete List of Authors:	Li, Jialu; University of Akron, Department of Chemical and Biomolecular Engineering Peng, Zhenmeng; University of Akron, Department of Chemical and Biomolecular Engineering

ARTICLE

Recent Advances of Reducible Metal Oxide Catalysts in C1 Reactions

Received 00th January 20xx,
Accepted 00th January 20xx

DOI: 10.1039/x0xx00000x

Jialu Li [a] and Zhenmeng Peng [a*]

Chemical conversion of one-carbon (C1) molecules to value-added chemicals and energy fuels has attracted increasing research interest in recent years, driven by the depletion concern of fossil fuel resources and the amplifying environmental issues caused by anthropogenic activities. In this mini-review, we introduce important C1 reactions in CO, CO_2, and CH_4 conversions via different approaches, including thermally, electrochemically and photochemically driven processes, and the catalysis mechanism of reducible metal oxide (RMO) materials for use in these reactions. We mainly summarize the latest research advances in RMO catalyst materials and their common functionality in these C1 reactions, discuss the current research status and challenges, and provide a perspective on future research directions and opportunities in this field.

Introduction

One-carbon molecules referred to as C1 chemicals, especially carbon monoxide (CO), carbon dioxide (CO_2), and methane (CH_4), are primarily sourced from fossil fuels, biomass, and organic wastes, having importance in chemical conversions. C1 chemistry has attracted dramatic research interests since the concerns on energy shortages and environmental problems have grown. Advanced technologies have been developed and investigated with an aim of transforming these inexpensive, abundant C1 feedstocks to value-added chemicals or energy fuels to meet sustainable development. Fischer-Tropsch (FT) process, water-gas shift reaction (WGSR), and steam methane reforming (SMR) are a few good examples from decades of fundamental studies in the lab to large-scale applications in industry. However, these traditional, thermal reaction routes are typically operated at elevated temperatures and pressures. This is largely due to the inert nature of CH_4 and CO_2 that makes it hard to activate and break C-H and C-O bonds and the difficulties of precisely controlling C-C coupling in CO transformation to target products.[1] Catalyst materials that attain good thermal stability are commonly used to adapt the harsh reaction conditions.[2,3] Recently, energy-effective strategies raised significant attention for C1 chemistry. Utilizing electrocatalysis and photocatalysis that apply electricity and photons as an additional driven force besides thermal energy, researchers have overcome the thermodynamic barriers and realized effective C1 conversions under a milder reaction condition.[4,5] Many of these studies are yet laboratory research, with remaining challenges in reaction activity improvement and selectivity control. Like the crucial role played in thermal C1 conversions, fundamental catalysis study and catalyst materials development are again at the core of the research to advance these new C1 technologies.

Reducible metal oxides (RMOs), like TiO_2, CeO_2, MnO_2, V_2O_5, etc., represent the most important group of C1 catalysts in reducible material categories. In the bigger picture, many oxygen-containing reducible compound catalysts could also be considered the broader family of reducible oxides based on their intrinsic reducibility of active sites, for instance, metal oxide hydroxides and mixed metal complexes (Figure 1). The RMO active sites would experience a valence oscillation in a catalysis cycle, typically accompanied by losing and regaining lattice oxygen in adjacency. The term "reducibility" depicts the ability for an active site to get reduced to a lower state, or the ability for a local defect vacancy to form during interaction with reacting species (Figure 1a).[6] Unlike RMO catalysts with reversibility of lattice oxygen redox, some other oxides, like SiO_2 and Al_2O_3, show a poor reducibility due to unfavoured thermodynamics and thus are generally considered as nonreducible oxides.[7,8,9] The interesting redox property creates prosperity in regard of research on excavating C1 reaction mechanisms, designing conversion routes, developing catalytic structures, and boosting catalysis performance using RMOs.[10] RMOs have often been found active in a same reaction via different approaches, i.e., thermally, electrochemically, and photochemically driven processes, implying common functionality of the RMO active sites regardless of how energy is administered to the reaction system.[11] Though there have been a large number of works investigating the unique structures and properties of RMOs with remarkable achievements in recent years,[12] the importance of systematic evaluation of this group of catalyst materials is underestimated. In contrast, there have been many excellent reviews on different catalyst materials, e.g., transition metals and alloys,[13,14] metal-organic frameworks (MOFs),[15,16] zeolite-based materials,[17,18] and single-atom catalysts.[19,20] Thus, our review in this article focuses primarily on RMO catalysts in some important C1 reactions that represents a good timing to summarize the new research progresses and fill the gap in the RMO field. In this mini-review, we introduce important C1 reactions in CO, CO_2, and CH_4 conversions, including thermal, electrochemical, and photochemical conversions, and summarize the latest understanding of RMO catalysis mechanisms and the catalyst material designs with the research challenges and opportunities being discussed.

[a] Department of Chemical, Biomolecular, and Corrosion Engineering, The University of Akron, Akron, OH 44325, United States.

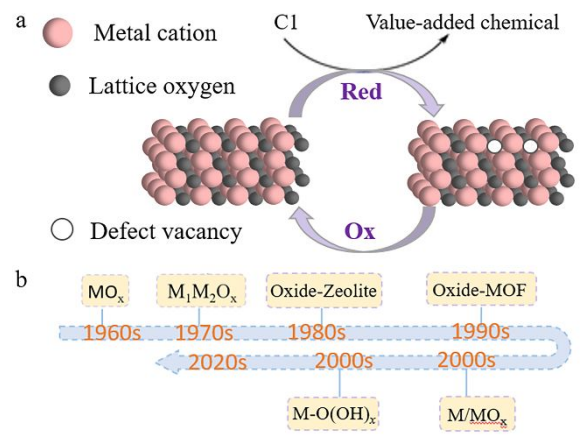

Figure 1. (a) Schematic illustration of RMO catalysts facilitating C1 conversion, (b) a list of RMO catalyst materials that have been discovered and studied in C1 conversion.

RMO catalysts in CO conversion

The conversion of CO, a colourless, odourless gas that can cause severe health and environmental hazards, has important applications in combustion engineering, gas purification, and fuel cell technologies (Figure 2). Owing to a weak permanent dipole moment ($\mu \approx 0.12$ D) and low excitation energy ($h\nu/k \approx 5.53$ K), CO is very chemically reactive with other reactants that lead to a variety of product molecules.[21] The research difficulties in CO conversion lie in avoiding overoxidation/overreduction for by-product formation.[22]

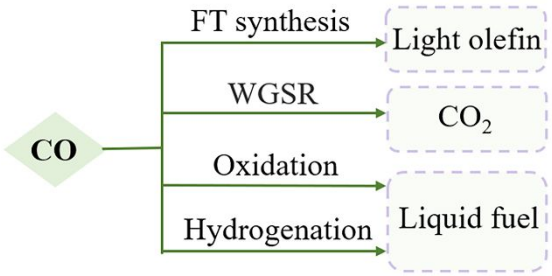

Figure 2. Major CO conversion routes. FT: Fischer-Tropsch; WGSR: Water-Gas Shift Reaction.

FT synthesis is a classic but complex method for CO hydrogenation to energy fuels and light olefins. An exceptionally selective olefin production can be achieved when RMOs are used, particularly in combination with zeolite which was attributed to confined C-C coupling by the zeolite acidic sites that remarkably prevent over-hydrogenation on RMO sites. Jiao et al. obtained as high as 94% C_2–C_4 hydrocarbons selectivity with 17% CO conversion, compared to the 58% benchmark selectivity, by discovering an OX-ZEO (Oxide-Zeolite) catalyst material (Figure 3a). An important active intermediate, ketene, was identified using highly sensitive synchrotron-based vacuum ultraviolet photoionization mass spectrometry (SVUV-PIMS) (Figure 3b).[23] Zn-Zr-O/SAPO-34, a mixed reducible oxide with zeolite, was reported with high selectivity toward methanol formation that suggested the bifunctional cooperation mechanism, with ZrO_2 activating CO and ZnO accelerating H_2 dissociative H_2 adsorption.[24] Besides zeolite, reducible oxides incorporated with a metal have been often used as cost-effective catalysts in CO conversions. Mejía et al. presented a large improvement in the reaction activity and 80% selectivity of long-chain hydrocarbons (C_{5+}) generation using TiO_2 and Nb_2O_5-supported Co–Ni catalysts. They found the oxides got partially reduced to suboxides that helped modulate the CO adsorption energy and benefitted the following CO dissociation process.[12]

Besides the thermal approach that can induce RMO active site state oscillation for facilitating CO conversion catalysis, previous studies have discovered many RMOs as effective catalysts in electrochemical and photochemical CO conversion reactions, with similar active site state oscillation although induced by these different energy administration approaches. Many RMOs could serve as photocatalysts or electrocatalysts based on their ability to harvest photons or transfer electronic charges. In electrocatalysis, electrode potential provides the driving force that would fulfil the thermodynamic CO conversion requirement. High reaction activity and selectivity can be achieved by adjusting the applied potential and tuning the RMO structure, i.e., the oxygen vacancy generation ability.[11] In photocatalysis, photon-excited holes/electrons would transfer to RMO active sites and facilitate CO conversion.[25] Although the specific CO reaction pathways in photochemical approach could be different from that in thermal approach, nevertheless RMOs function similarly, with oxygen vacancy consumption and regeneration being essential to complete catalysis cycles.[26] For instance, Co/Co_3O_4, Fe/Fe_3O_4, Ni/NiO_x, and Ni_2P/TiO_2 catalysts were studied in solar-driven CO conversion.[27,28,29,30] Scanning tunnelling microscopy (STM) characterizations suggested that oxygen vacancies on RMO surfaces are the primary CO adsorption and activation sites,[31] and density functional theory (DFT) calculations suggested that RMO phase contributed to tuning the electronic properties of metallic components, enhancing C-C coupling toward olefins generation and weakening hydrogenation toward alkanes. These effects collectively resulted in selective production of light olefins.[27,28,29] A summary of those RMO catalysts on FT conversion route is shown in Table 1.

In WGSR, CO reacts with water and produces H_2 and CO_2. Being exothermic allows effective CO transformation with high conversion and mild operation conditions, this reaction offers an important process for hydrogen production and purification. Reducible metal sulfides and phosphides (MS_x, MP_x), a subgroup of the broader reducible material family, have been widely exploited for their unique catalytic properties in WGSR.[32,33] According to the literature, MS_x would generate sulfur vacancies, similar to oxygen vacancies generated in reducible oxides, which interact with reacting species and facilitate intermediate and product generation besides preventing side reactions and sintering.[34] Besides WGSR synthesis, MoP can be applied on CO hydrogenation for alcohols, methane, and other hydrocarbons production under room temperature and atmosphere pressure.[35]

CO oxidation is an important, widely applied reaction in practice for controlling CO emission by converting it to CO_2. Many RMOs, like the oxides of Mn, Ce, Cu, Ni, Co, and Ti elements, are good catalyst candidates considering their earth abundance thus a low cost and interesting structure-sensitive catalytic properties.[36,37,38,39] This reaction was discovered to follow the Mars-van Krevelen mechanism on RMOs, with the catalyst surface being partially reduced by adsorbed CO and getting re-oxidized back to its initial state by O_2 in a catalysis cycle (i.e., RMOs render a consumption and rejuvenation of oxygen vacancies repeatedly) (Figure 4).[40] Pan et. al. investigated the activity property of different RMOs using a combination of experimental measurements and computational simulations. They discovered the RMO activity can be depicted by two governing parameters, i.e., work function and work function oscillation of catalyst materials.[41] The reducibility of RMO and the corresponding the activity property in CO oxidation can be regulated by substitution or incorporation with other cations.[42] For example, the study of dopants modified TiO_2 found a boost of activity in CO oxidation, and the in-situ Fourier-transform infrared spectroscopy (FT-IR) and X-ray

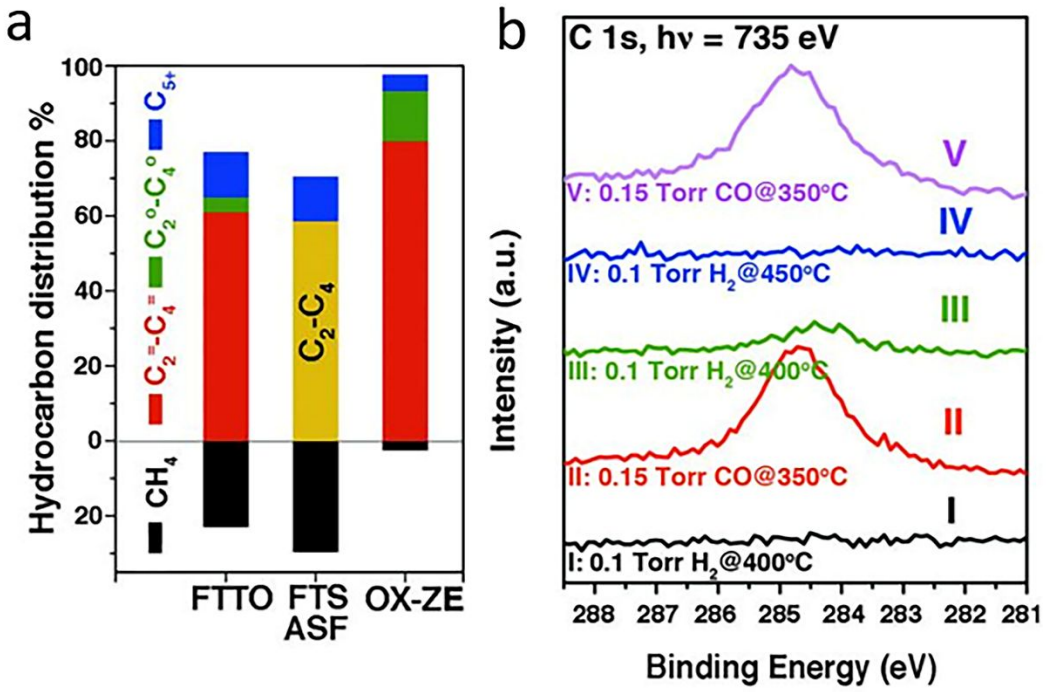

Figure 3. (a) Hydrocarbon distribution in OX-ZEO in comparison to that reported for Fischer-Tropsch to olefins (FTTO) and that in Fischer-Tropsch synthesis (FTS) predicted by the Anderson-Schulz-Flory (ASF) model at a chain growth probability of 0.46 with the yellow bar representing selectivity of C_2–C_4 hydrocarbons. (b) In situ study of syngas conversion over $ZnCrO_x$ by SVUV-PIMS at hυ = 9.72 eV. The insets display the signals of *m/z* = 42.01 (ketene) and *m/z* = 42.05 (propene) detected at hυ = 9.72 and 11.40 eV, respectively. This figure has been adapted from ref. 23 with permission from AAAS, copyright 2016.

photoelectron spectroscopy (XPS) characterizations confirmed the crystal phase of oxides has an impact on catalytic performance.[43] Recently, Fe_2O_3 modified with Pt single atoms was reported with 100% CO conversion at about 70 °C. In this work, monodispersed Pt atoms were found to bring more structure defects to Fe_2O_3 that led to the generation of more oxygen vacancy sites catalyzing CO oxidation.[44] Some mixed RMOs, like hopcalite ($CuMnO_x$) and modified hopcalite, were also studied and exhibited CO oxidation activity at room temperature.[45,46] It was concluded that the lattice oxygen associated with Cu and the mobility of lattice oxygen with Mn enabled the unique property of hopcalite.

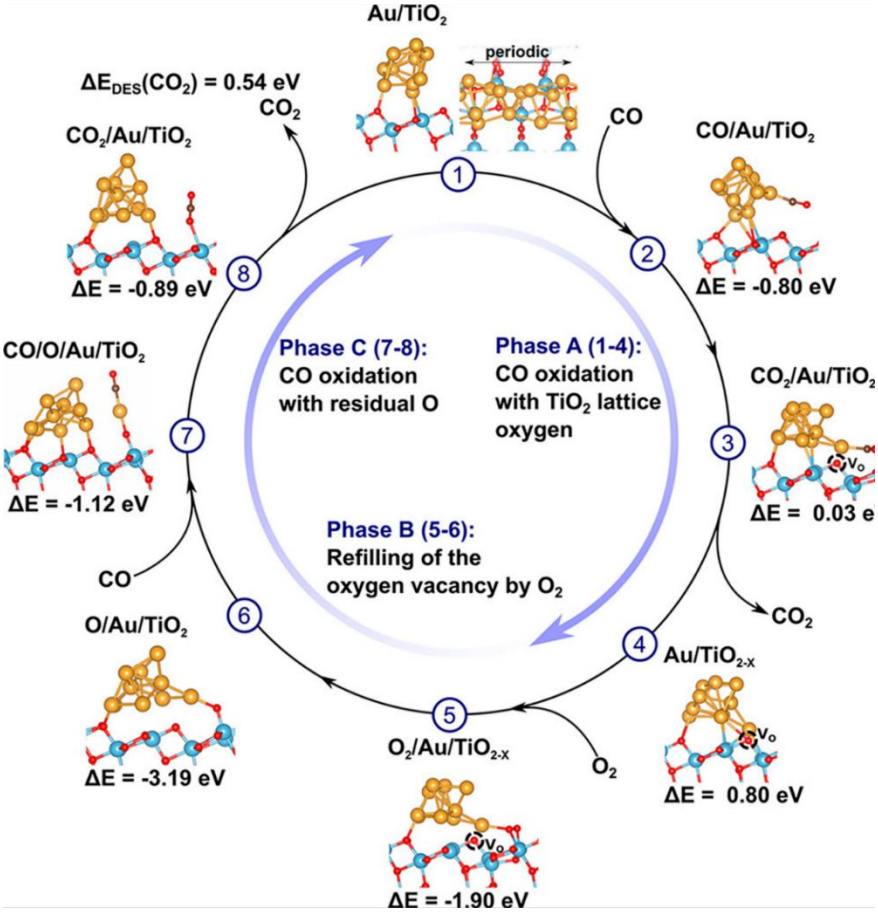

Figure 4. Possible catalytic cycle for CO oxidation on Au_{10}/TiO_2 involving the formation of a single oxygen vacancy and one oxygen adatom. In phase A, a titania lattice oxygen is abstracted by CO, forming CO_2 and an oxygen vacancy. In phase B, the oxygen vacancy is re-oxidized by O_2, leaving an oxygen adatom O_{ad} at the Au/TiO_2 interface. In phase C, the oxygen adatom O_{ad} is abstracted by CO, under formation of the second CO_2 molecule. This figure has been adapted from ref. 40 with permission from American Chemical Society, copyright 2018.

Table 1. A summary of RMO catalysts and the performance in FT synthesis.

	Reaction conditions					Product selectivity		
catalysts	T (K)	P (MPa)	GHSV (ml/g_{cat} h)	H_2/CO	X_{CO} (%)	C1	C2−C4	C5+
$ZnCrO_x$/ MSAPO	673	2.5	5143	2.5	17	2	94	4[23]
$ZrZnO_x$/ SAPO	673	1	3600	2	9.5	6	92	2[24]
MnO_x/ SAPO	400	2.5	4800	2.5	7	1	94	5[47]
Co−Ni/ TiO_2	493	0.1	20000	2	4.4	9	15	76[12]
Co−Ni/ Nb_2O_5	493	0.1	20000	2	3.7	9	15	76[12]
Fe_0-FeO_x/ZnO-Al_2O_3	273 (visible light)	0.18	3000	3	12	39	50	11[27]
Co-Co_3O_4/ZnO-Al_2O_3	273 (Xe light)	0.18	6000	3	15	48	42	10[28]
Ni/NiO_x	273 (Xe light)	0.08	/	3	28	41	38	21[29]
Ni_2P/TiO_2	478 (Xe light)	0.18	6000	3	13.3	25	47	28[30]

RMO catalysts in CO_2 conversion

CO_2 is a natural greenhouse gas and closely connects to human living. Excess CO_2 emissions have been generated from anthropogenic activities that result in irreversible environmental problems.[48] CO_2 conversion offers an imperative strategy to regulate CO_2 emissions and has attracted significant research interests. The major challenges in CO_2 conversion are to overcome the coke effect, particularly for high-temperature reactions, and to activate the thermodynamically uphill reactions.[49]

Thermal-driven CO_2 hydrogenation, using H_2 as the reductant, includes four important reactions: reverse water gas shift reaction (RWGS), methanation, FT reaction, and methanol synthesis (Figure

5).[50,51,52] RMOs embraced by other elements, like perovskite and noble metal, were found with improved catalytic properties, which was attributed to a modification in oxygen mobility by reorganizing the defective oxide structure.[653,54,55] Many RMO materials can serve as tandem catalysts in the CO_2-CO chemistry networks that help control reaction pathways in two sequential reactions, avoiding intense energy consumption in one-step conversion,[56] and therefore, the catalyst choice and mechanisms for CO_2 conversion share some similarities with CO conversion.

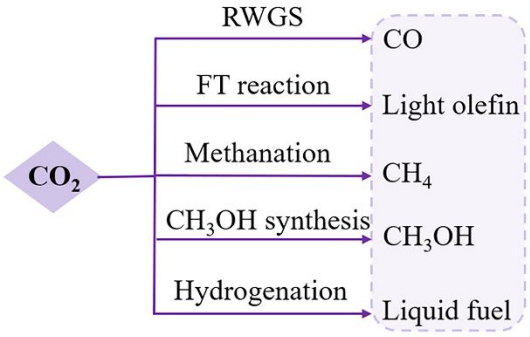

Figure 5. Major CO2 conversion routes. RWGS: Reverse Water-Gas Shift; FT: Fischer-Tropsch.

CO_2 transformation for methanol synthesis using $Cu/ZnO/Al_2O_3$ has attracted substantial attention over decades due to its remarkable properties in a mild temperature range (475 to 575 K).[57] Later on, Martin et al. found In_2O_3/ZrO_2 catalyst with superior activity and stability and 100 % methanol selectivity in the reaction,[58] which attracted more investigations on In_2O_3.[59] The introduction of ZrO_2 was found to improve the dispersion of In_2O_3 nanoparticles that benefits with more active sties and meanwhile to stabilize them from sintering.[58] A following work from the same group unveiled the geometric and interfacial effects of In_2O_3/ZrO_2. The monoclinic active phase of ZrO_2 support was identified to help epitaxial alignment of In_2O_3 and form monoclinic polymorph that would generate tensile strain and form an improved diverse number of oxygen vacancies.[60] Yao et al. reported the study of Cu-In-Zr-O mixed oxide and near 80% methanol selectivity under mild conditions. Metallic Cu sites were found responsible for H_2 dissociation and active hydrogen formation that promote vacancies bonding with intermediate and hydrogenation kinetics toward methanol formation. In situ diffuse reflectance infrared Fourier transform spectroscopy (DRIFTS) studies suggested the formate-methoxy-methanol formation pathway on this mixed reducible oxide catalyst (Figure 6).[61] The mechanism of the metal promotion effect was further illustrated in the study of Pd/In_2O_3.[62] Frei et al. reported that well-dispersed Pd atoms on In_2O_3 possessed metal-support interactions that would modify the electronic properties of In_2O_3. Meanwhile, the stabilized low-nuclearity Pd was found to facilitate H_2 splitting with a suppression of undesired CO formation. Both XPS O1s and solid-state nuclear magnetic resonance (NMR) spectroscopy indicated generation of more abundant oxygen vacancies by substituting Pd in In_2O_3. Co-precipitated catalyst (CP) and dry impregnation catalyst (DI), synthesized with different methods, were demonstrated having a different impact on CO_2 hydrogenation to methanol performance, which was attributed to a difference in the defect local environment, wherein CP catalyst exhibited a good activity (0.96 $g_{MeOH}\ h^{-1}\ g_{cat}^{-1}$) and retained an excellent stability for 500 h.[62] More recently, a ternary $Pd\text{-}In_2O_3\text{-}ZrO_2$ catalyst with a superior performance (1.3 $g_{MeOH}\ h^{-1}\ g_{cat}^{-1}$) and improved metal utilization was investigated, with a lower apparent activation energy being responsible for the more facile methanol generation kinetics. Aberration-corrected scanning electron microscopy (AC-STEM) and energy-dispersive X-ray spectroscopy (EDX) characterized mixed ZrO_2 phase on individual particles and indicated that pure monoclinic ZrO_2 structure was not indispensable for high-performance CO_2 conversion. Electron paramagnetic resonance spectroscopy (EPR) was found as a powerful technique for helping interpret catalyst performance in CO_2 hydrogenation because EPR is capable to quantify oxygen vacancy and analyse its dynamics (Figure 7).[63] Besides the cationic component incorporation effect, an anionic P element incorporation into In_2O_3 was reported to regulate RMO catalyst activity and selectivity by tuning the catalyst surface adsorption configuration. In situ DRIFTS spectra indicated the In–P bond undermined oxygen vacancy formation on In_2O_3 surface, and thus CO_2 adsorbed to alternative sites and favoured CO generation. In comparison, on a pristine In_2O_3, CO_2 took up oxygen vacancy and bonded to the adjacent site, leading to preferential methanol generation (Figure 8).[64]

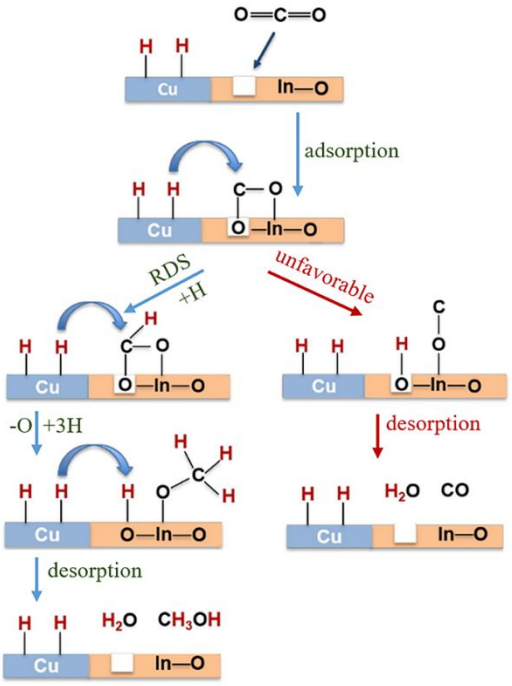

Figure 6. Schematic representation of Cu-In_2O_3 synergy on $Cu_{0.25}\text{-}In_{0.75}\text{-}Zr_{0.5}$-O for methanol synthesis Reaction condition: T = 250 °C, P = 25 bar, GHSV = 18000 ml/(g_{cat}·h). RDS: rate-determining step. This figure has been adapted from ref. 61 with permission from Elsevier, copyright 2019.

CO_2 can also be directly converted to other valuable chemicals, such as ethyl alcohols, dimethyl ether (DME), carboxylic acids, and dimethyl carbonate. For example, in the CO_2-to-DME thermal reaction 65.1% DME selectivity was achieved using a Cu–In–Zr–O/ SAPO catalyst. The proximity of the RMO (Cu–In–Zr–O) particles with the zeolite (SAPO) particles made a dramatically difference to the reaction mechanism, with the methoxy-DME shortcut pathway being followed when the two components were in close proximity.[65]

Photocatalytic and electrocatalytic CO_2 reduction have been investigated as alternative methods that can utilize renewable solar/electrical energy to drive the reactions in the presence of RMO catalysts. TiO_2, Co_3O_4, Ga_2O_3, ZnS, and SnO_2 were discovered with interesting activity property towards formate formation.[66,67] SnS_2, MoS_2, and Bi_2WO_6 were reported as effective catalyst for alcohol generation.[68,69]

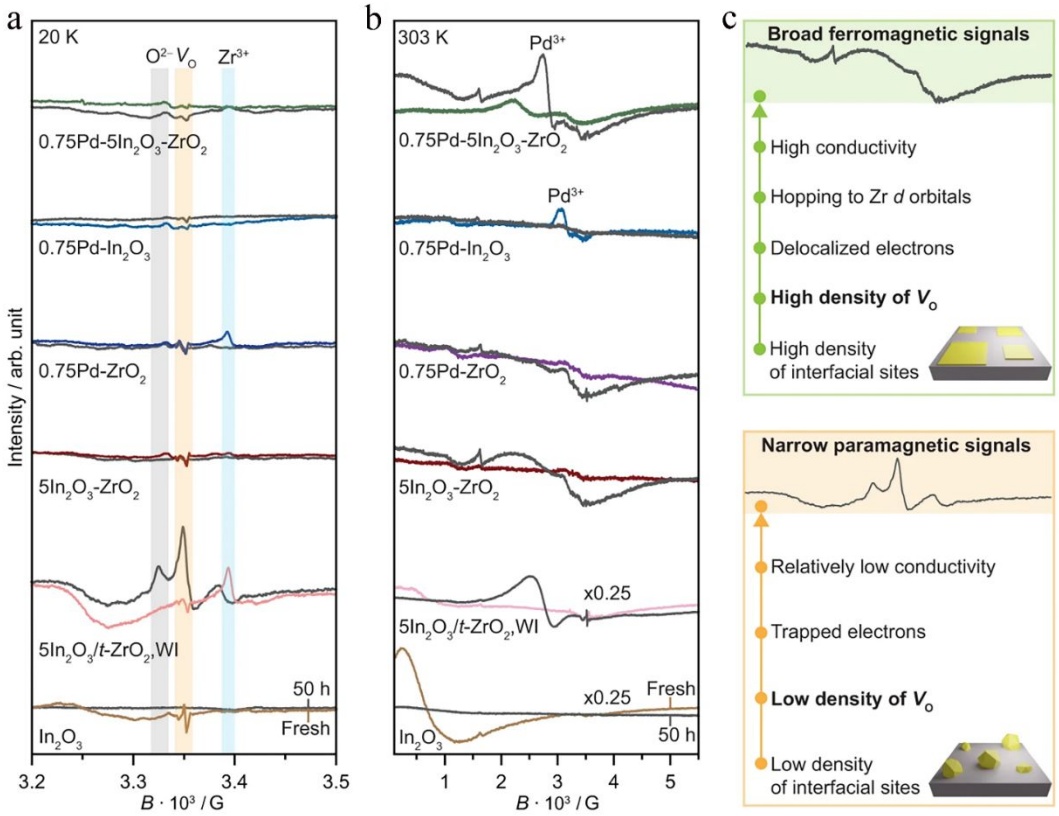

Figure 7. Ex situ EPR spectra of In_2O_3-based catalysts prepared by FSP and WI in fresh form and after CO_2 hydrogenation for 50 h measured at (a) 20 K and (b) 303 K. (c) Scheme describing the nature of EPR signals generated from catalysts displaying distinct densities of interfacial sites and oxygen vacancies. Activation conditions: T = 553 K, P = 5 MPa, H_2/CO_2 = 4, and $GHSV$ = 48,000 $cm^3\ h^{-1}\ g_{cat}^{-1}$. This figure has been adapted from ref. 63 with permission from Nature, copyright 2022.

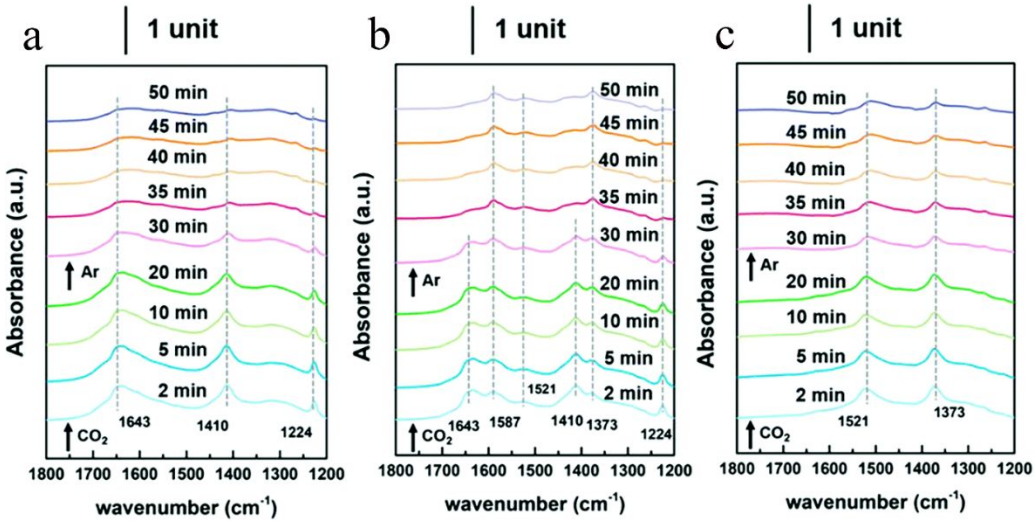

Figure 8. Time-evolved in situ DRIFTS spectra (1800–1200 cm^{-1}) of CO_2 adsorption experiments on In_2O_3 materials. (a) P–In-0, (b) P–In-2 and (c) P–In-3.5 (0, 2, and 3.5 represents molar ratio between P and In). This figure has been adapted from ref. 64 with permission from Royal Society of Chemistry, copyright 2021.

RMO catalysts in CH_4 conversion

Selective conversion of methane, the main component of natural gas and an abundant non-renewable resource, to value-added chemicals and liquid fuel remained a grand challenge in the past

century. The challenge was largely caused by the stable characteristic of the CH_4 molecule that raises difficulty to overcome the 439.3 kJ·mol^{-1} dissociation energy for C-H bond activation and cleavage, and by the difficulty to control the reaction extent from over-oxidation.[70] As of date, SMR has been applied as an important industrial process for converting CH_4 into syngas that can be further used as the feedstock for value-added chemicals production. The SMR is endothermic and requires high temperature and pressure conditions (typically over 973 K and 15 bar) for overcoming the thermodynamics and improving the kinetics.[71] Direct CH_4 conversion to value-added chemicals (Figure 9), which can not only simplify the overall processes but also is more economically beneficial, theoretically feasible, and has attracted significant, long-time attention.

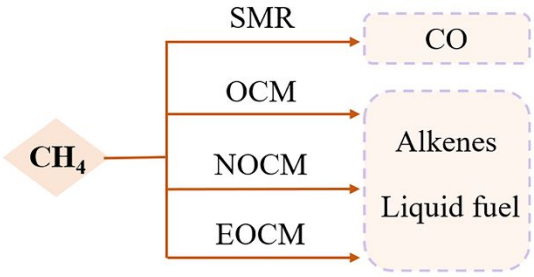

Figure 9. Major CO conversion routes. SMR: Steam Methane Reforming; OCM: Oxidative Methane Conversion; NOCM: Nonoxidative Methane Conversion; EOCM: Electrochemical Oxidative Conversion of Methane.

Oxidative conversion of methane (OCM) offers a route that can directly convert CH_4 into alkenes and oxygenates by reacting with oxidants like O_2 and H_2O_2. A recent study showed that CH_4 was oxidized to methanol using a Fe-containing zeolite structure, with the Fe sites being identified as active centers that undergo Fe(II)/Fe(IV) redox cycles in catalysis.[72] In another study, formic acid production with 90% selectivity was reported by oxidizing CH_4 with H_2O_2 using a FeN_x/C-5-700 catalyst, in which the reducible FeN_x was found to provide the active sites for hydroxyl radical generation and OCM.[73] Although the use of oxidants other than O_2 was often discovered with better reaction kinetics and selectivity control, it would raise a cost-effectiveness concern for large-scale applications. When O_2 is used as the oxidant, the OCM reaction on RMO catalyst follows the typical RMO catalysis mechanism, with the active sites getting reduced by reacting with CH_4 and getting re-oxidized by O_2 for regeneration in a catalytic cycle. A variety of RMO materials, like IrO_2, CeO_2, TbO_x, TiO_2, PdO, La_2O_3, and mixed oxide $MnTiO_3$, have been explored for the catalytic properties in the OCM reaction.[74,75,76] For example, PdO was found effective in CH_4 activation following the dissociative adsorption mechanism, in which stoichiometrically unsaturated Pd sites and surrounding oxygen vacancies are considered as the active sites.[77] Besides, La_2O_3 was reported with high hydrocarbon production selectivity and CeO_2 showed high OCM activity. Meanwhile, the catalytic properties of RMOs can be altered by modifying the catalytic structure. Improvements in both the activity property of La_2O_3 and the selectivity property of CeO_2 in OCM were achieved by doping the two materials.[78] More recently, Liu et al. reported OCM to methanol with 95% selectivity on CeO_2/Cu_2O/Cu(111) catalyst at low temperature in presence of water, the introduction of which was found to introduce hydroxyl species that blocks O_2 dissociation and favors the hydrogenation of methoxy groups.[79]

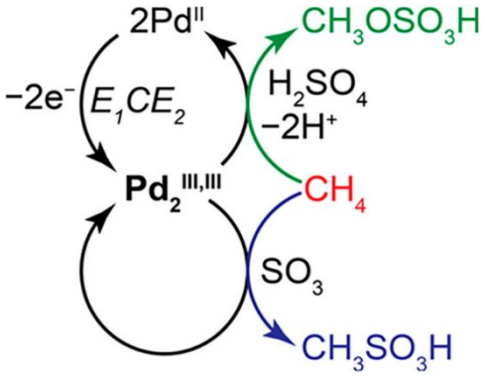

Figure 10. Proposed mechanism for electrochemical methane functionalization by a putative $Pd_2^{III,III}$ intermediate. Green and blue arrows indicate faradaic and nonfaradaic reaction pathways, respectively. This figure has been adapted from ref. 83 with permission from American Chemical Society, copyright 2017.

Non-oxidative conversion of methane (NOCM) provides a potentially more cost-effective, eco-friendly route for CH_4 utilization, considering the challenge to inhibit CO_2 generation in OCM that sabotages the carbon use efficiency and no such concern in NOCM. Earlier in 2015, Gao et al. reported the design of Mo oxide monomer anchored on Al sites in zeolite framework as a catalyst in NOCM. It was found that the oxide was firstly transformed into carbide species by reacting with CH_4 under the reaction conditions and then the Mo-C served as active sites that catalyzed C-H bond scissoring and methyl intermediate generation.[80] Compared to thermal OCM and NOCM reactions, electrochemical oxidative conversion of methane (EOCM) utilizes electrode potential as an additional parameter to drive the reaction that would allow its occurrence under more mild conditions. There have been active studies of EOCM utilizing solid oxide fuel cell (SOFC) in the higher temperature range, in which O_2 is electrochemically reduced to O^{2-} at the cathode and O^{2-} migrates to the anode that electrochemically reacts with CH_4 for oxygenates generation. CeO_2 was often used as an anode RMO catalyst owing to its exhibited good ionic conductivity and high CH_4 oxidation activity.[81,82] Surendranath et al. reported the use of Pd-complex in concentrated sulfuric acid electrolytes in EOCM, with the Pd^{II} ions serving as the active sites that undergo $Pd^{II}/Pd_2^{III,III}$ cycle to catalyze generation of CH_3OSO_3H and CH_3SO_3H species (Figure 10). The interchangeable Pd valence states during the catalytic cycle were evidenced by cyclic voltammetry (CV) and in situ UV–vis spectroelectrochemistry.[83] Pt-containing complexes were also found effective and catalyzed EOCM with Pt^{II}/Pt^{IV} reducible sites.[84] V_2O_5 has also attracted attempts among RMO catalysts in EOCM for its interesting activity property in the lower temperature range,[85,86] however, the low product selectivity remained an issue. More recently, Li et al. conducted a systematic study of EOCM toward ethanol on iron-nickel hydroxide (Fe-Ni-OH) nanosheet catalyst under room temperature and atmospheric pressure conditions (Figure 11). They observed an interesting Fe-Ni-OH composition effect on the catalytic properties, with $Fe_3Ni_7(OH)_x$ showing the best performance and exhibiting excellent activity with 0.26 s^{-1} turnover frequency (TOF $_{ethanol}$) and 87% ethanol selectivity. The in-situ ATR-FTIR experimental results and DFT simulations suggested in situ generated $Ni^{III}OOH$ as the active sites following the

RMO catalysis mechanism, with the Fe incorporation modifying the local configuration of active sites that promote the EOCM kinetics by lowering the energy barrier.[87] A variety of other RMO catalysts, e.g., NiO_2,[88,89] Co_3O_4,[90] and $NiCO_2O_4$,[91] have also been discovered with interesting properties in EOCM and were investigated in literature (Table 2).

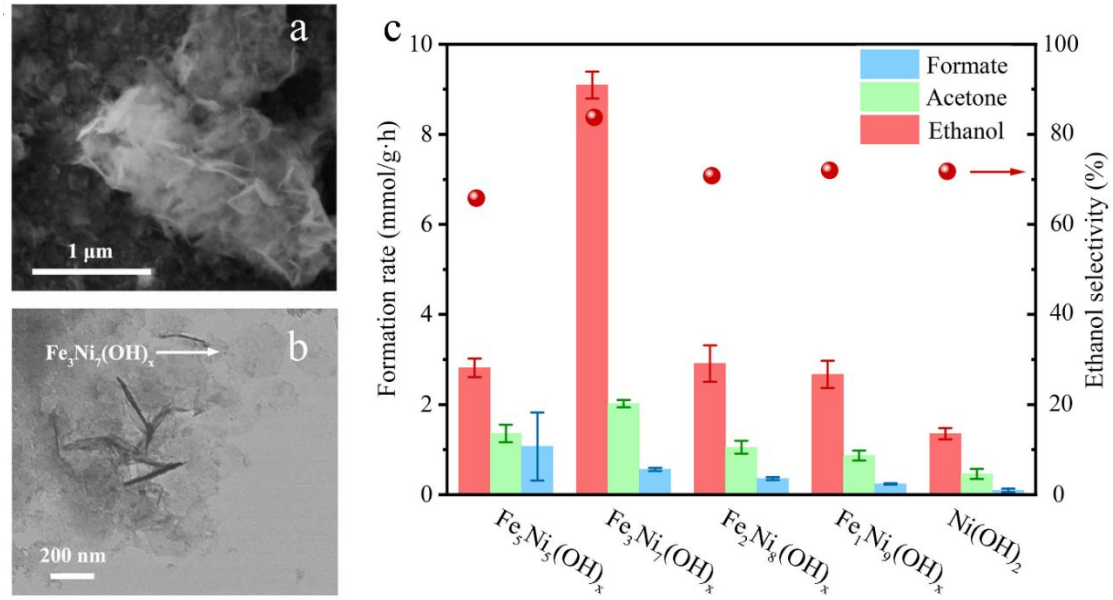

Figure 11. (a) SEM (scanning electron microscope) images (b) TEM (transmission electron microscopes) images of the synthesized Fe-Ni-OH nanosheets. The arrow points to individual symmetric hexagonal shape nanosheet. (c) The measured formation rate of different products and ethanol selectivity using different Fe-Ni-OH catalysts. This figure has been adapted from ref. 87 with permission from Elsevier, copyright 2022.

Table 2. A summary of RMO catalysts and the performance in electrocatalytic CH_4 conversion.

Catalyst	T (K)	Pressure (MPa)	Electrolyte	Potential (V)	Product
$Pd^{II}/Pd_2^{III,III}$	375	3.5	20% SO_3/H_2SO_4	2	methanol precursors[83]
Cu/CeO_2	973	0.1	yttria-stabilized zirconia (YSZ)	0.4-1.1	CO_2[76]
$Pt^{II}/^{IV}$	403	3.5	10 mM NaCl, 0.5 M H_2SO_4	0.829 (V vs. SHE)	methanol (80% selectivity)[84]
V_2O_5/SnO_2	373	200	$Sn_{0.9}In_{0.1}P_2O_7$	0.9	methanol (88 % selectivity)[85]
V^V/V^{IV}	273	0.1	98% H_2SO_4	2.3 (V vs. Hg_2SO_4/H)	methyl bisulfate (81% selectivity) [86]
Fe-Ni-OH	273	0.1	0.1 M NaOH	1.46 (V vs. RHE)	ethanol (87% selectivity)[87]
$NiO-ZrO_2$	313	0.1	0.1M Na_2CO_3	1.8 (V vs. SCE)	isopropanol, acetate/acetic acid acetone, ethanol, and formate/formic acid[88]
Rh/ZnO	273	0.1	0.1 M KOH	2.2 (V vs. RHE)	ethanol (85% selectivity)[89]
Co_3O_4/ZrO_2	273	0.1	0.5 M Na_2CO_3	2.0 (V vs. Pt)	2-propanol and 1-propanol[90]
ZrO_2-$NiCo_2O_4$	273	0.1	0.5 M Na_2CO_3	2.0 (V vs. Pt)	propionic acid, acetic acid and acetone[91]

Outlook and Perspective

Sustainable C1 conversion to value-added chemicals and energy fuels offers a promising solution to help alleviate the energy shortages and slow down the environmental change. In this review, we have reviewed the important reactions for C1 molecules (CO, CO_2, and CH_4) and summarized the recent progresses in researching RMO catalyst materials for these reactions. The research progresses have significantly advanced C1 chemistry and RMO catalyst development and lie as a foundation stone to guide new catalyst research activities in this field. In the meantime, challenges remained in the RMO catalysis research, particularly in the fundamental study of catalysis

mechanisms and in the rational discovery of new materials with desired catalytic properties.

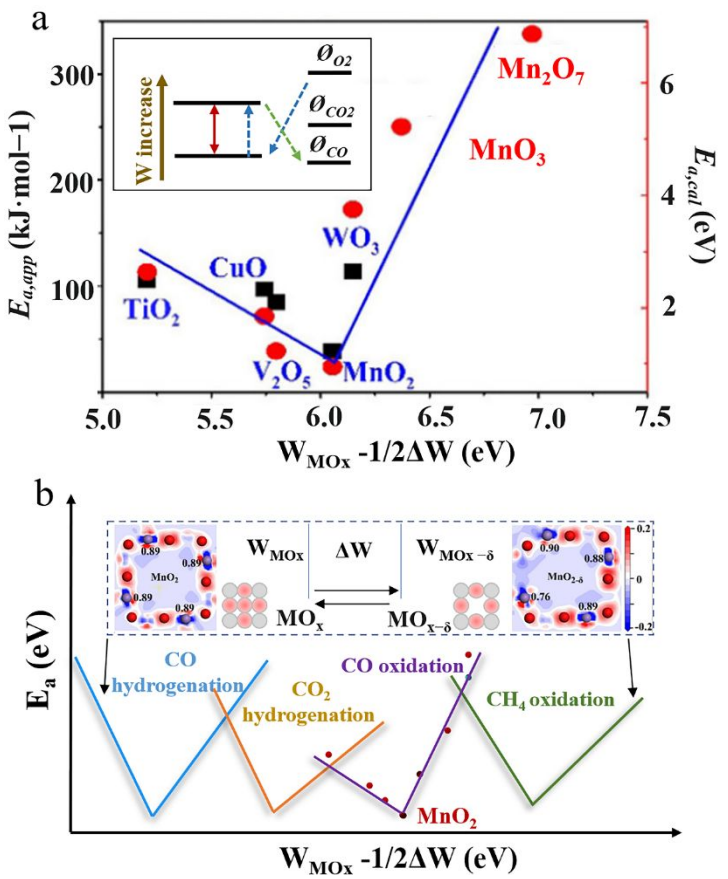

Figure 12. (a) Inverted volcano correlation of (W_{MOx}-ΔW/2) with $E_{a,app}$ (black square) and $E_{a,cal}$ (red dot). Inset: relative work function and potential levels of RMOs and reacting species. This figure has been adapted from ref. 41 with permission from Wiley-VCH Verlag GmbH & Co. KGaA, copyright 2019. (b) Illustration of (W_{Mox} -1/2ΔW) as possible RMO material parameter for depicting the catalytic activity property in different C1 conversion reactions. W_{MOx} represents work function, ΔW represents oscillation of work function, and E_a represents activation energy.

At the mechanistic study level, previous studies have discovered the general RMO catalysis mechanism in C1 reactions, in which reducible cations and surrounding vacancies on the RMO surface serve as the active sites. In C1 oxidation, the active sites would react with C1 molecules to generate intermediates/products, accompanied with a reduction in the active sites, i.e., cation valence lowering and vacancy formation. The reduced active sites would then react with oxidant for regeneration to the initial state that completes a catalysis cycle. In C1 reduction, the active sites would be reduced by reductant to a lower state, which would then react with C1 molecules for product generation and meanwhile get oxidized to the initial state. However, it remained challenging to characterize the exact structural configuration and evolution of working active sites and the interactions with reacting species.

At the RMO catalyst research level, different material parameters, like composition, crystallinity, and reducibility, have been found with dramatic effects on the catalytic properties. This implies the existence of RMO structure-property relationship that would have significances both in fundamental interests to understand RMO catalysis properties and in practical applications to guide new catalyst development. However, as of date, the exact relationship between RMO material parameters and the catalytic properties remained elusive. The RMO catalyst discovery and research relied still largely on experiences with trial and error. A lack of the exact RMO structure-property relationship has been a significant roadblock in new catalyst research and development.

Previous studies have witnessed considerable efforts to explore the RMO structure-property relationship. The research efforts can be traced back to early twentieth century, with the Bronsted-Evans-Polanyi principle (also referred to as the Bell-Evans-Polanyi or Evans-Polanyi-Semenov principle) finding the difference in activation energy between two reactions of the same family has a proportional relationship with the difference in their enthalpy of reaction.[92] In the following years, researchers continued to study on this topic and published a series of works on proposing semiquantitative property-activity relationships to describe RMO catalysis. Most notably, the catalyst activity property was discovered to follow a decent volcano relationship with the enthalpy of transition from a lower to a higher oxidation state for oxides (ΔH_F).[93] The reaction activation energy was found to show a linear correlation with the oxygen vacancy formation energy of oxides (ΔE_{vac}), also referred to as the surface

reducibility. These findings confirmed that the reaction properties are indeed controlled and describable by certain governing parameters of reducible oxides. However, it needs to be noted that these used descriptors are properties of oxide materials, but not at the level of intrinsic oxide material parameters that can be experimentally measured. More recently, RMO material parameters like work function[94] and occupancy of the e_g-symmetry orbital[95] were examined for use as a descriptor for depicting the reaction activity property. Pan et. al. developed a theoretical model using RMO work function (W) and oscillation of work function (ΔW) for depicting the activity property in CO oxidation as a probe reaction (Figure 12).[41] This model considered the oscillation of active sites between different oxidation states and suggested the material parameters associated with both states collectively control the activity property. To certain extent, the used ΔH_F and ΔE_{vac} material properties and their correlation with the reaction properties in previous studies already revealed the importance of both active site states during RMO catalysis. The established inverted volcano correlation between (W- ΔW/2) and the activation energy by Pan et. al. was in decent consistence with the experimental results (Figure 12a). This theoretical model could possibly be extended to many other RMO catalysis processes. Different C1 reactions, like CO hydrogenation, CO_2 hydrogenation, and CH_4 oxidation, on RMO catalysts would follow a similar structure-activity property correlation, with the optimal (W- ΔW/2) requirement being different (Figure 12b). Previous studies have suggested that regardless of how energy is administered to the reaction system, i.e., via thermal, electrochemical, and photochemical approaches, RMO catalysts follow the same function mechanism, with the active site oscillation accompanied by oxygen vacancy consumption and regeneration to complete a catalysis cycle. In this regard, the discovered RMO structure-property relationship in thermal C1 reactions could be possibly extendable to help study electrochemical and photochemical reaction systems.

With rapid developments in advanced characterization techniques and in computational chemistry,[96,97] new approaches have been and will be more extensively utilized to further the RMO catalysis understanding. For example, in situ/operando tools that can spatially and temporally identify and monitor RMO active site,[63] atomic-level characterizations that can define the active phase structure,[62] and in-depth analyses using electron spin resonance (ESR) spectroscopy, laser-induced fluorescence (LIF), and atomic resonance absorption spectroscopy (ARAS) that can detect active, short-life intermediates[98] are expected to provide insightful experimental evidence and yield new knowledge of the RMO active site and C1 catalysis mechanisms. These fundamental understandings would also help to identify the governing RMO material parameters and establish exact RMO structure-catalytic property relationships. This would lead to more accurate theoretical models that can not only help to understand RMO catalysis but also provide guidance for new catalyst research and development. Rational RMO catalyst design and high-throughput material screening with a combined theoretical and experimental approach for desired properties will become possible, which will lead to more efficient C1 chemical conversions to targeted products and eventual applications.

Author Contributions

Dr. Zhenmeng Peng provided guidance, conceived, and planned the main context. Jialu Li did literature research and wrote the paper. All authors provided critical feedback and helped shape, finalize the manuscript.

Conflicts of interest

There are no conflicts to declare.

Acknowledgements

The National Science Foundation Support (grant number 1955452) is acknowledged.

Reference

1 N. J. Gunsalus, A. Koppaka, S. H. Park, S. M. Bischof, B. G. Hashiguchi and R. A. Periana, Homogeneous functionalization of methane, *Chem Rev*, 2017, **117**, 8521–8573.

2 Y. Song, E. Ozdemir, S. Ramesh, A. Adishev, S. Subramanian, A. Harale, M. Albuali, B. A. Fadhel, A. Jamal and D. Moon, Dry reforming of methane by stable Ni–Mo nanocatalysts on single-crystalline MgO, *Science (1979)*, 2020, **367**, 777–781.

3 P. R. Ellis, D. I. Enache, D. W. James, D. S. Jones and G. J. Kelly, A robust and precious metal-free high performance cobalt Fischer–Tropsch catalyst, *Nat Catal*, 2019, **2**, 623–631.

4 J. Xie, R. Jin, A. Li, Y. Bi, Q. Ruan, Y. Deng, Y. Zhang, S. Yao, G. Sankar and D. Ma, Highly selective oxidation of methane to methanol at ambient conditions by titanium dioxide-supported iron species, *Nat Catal*, 2018, **1**, 889–896.

5 Y. Zhou, L. Zhang and W. Wang, Direct functionalization of methane into ethanol over copper modified polymeric carbon nitride via photocatalysis, *Nat Commun*, 2019, **10**, 506.

6 A. Ruiz Puigdollers, P. Schlexer, S. Tosoni and G. Pacchioni, Increasing oxide reducibility: the role of metal/oxide interfaces in the formation of oxygen vacancies, *ACS Catal*, 2017, **7**, 6493–6513.

7 J. Wang, R. You, C. Zhao, W. Zhang, W. Liu, X.-P. Fu, Y. Li, F. Zhou, X. Zheng and Q. Xu, N-coordinated dual-metal single-site catalyst for low-temperature CO oxidation, *ACS Catal*, 2020, **10**, 2754–2761.

8 C. H. Wu, C. Liu, D. Su, H. L. Xin, H.-T. Fang, B. Eren, S. Zhang, C. B. Murray and M. B. Salmeron, Bimetallic synergy in cobalt–palladium nanocatalysts for CO oxidation, *Nat Catal*, 2019, **2**, 78–85.

9 Y. Wang, P. Ren, J. Hu, Y. Tu, Z. Gong, Y. Cui, Y. Zheng, M. Chen, W. Zhang and C. Ma, Electron penetration triggering interface activity of Pt-graphene for CO oxidation at room temperature, *Nat Commun*, 2021, **12**, 5814.

10 A. R. Puigdollers and G. Pacchioni, CO oxidation on Au nanoparticles supported on ZrO2: role of metal/oxide interface and oxide reducibility, *ChemCatChem*, 2017, **9**, 1119–1127.

11 S. Xie, W. Ma, X. Wu, H. Zhang, Q. Zhang, Y. Wang and Y. Wang, Photocatalytic and electrocatalytic transformations of C1 molecules involving C–C coupling, *Energy Environ Sci*, 2021, **14**, 37–89.

12 C. Hernández Mejía, J. E. S. van Der Hoeven, P. E. de Jongh and K. P. De Jong, Cobalt–Nickel Nanoparticles Supported on Reducible Oxides as Fischer–Tropsch Catalysts, *ACS Catal*, 2020, **10**, 7343–7354.

13 W. Zhu, Y.-J. Zhang, H. Zhang, H. Lv, Q. Li, R. Michalsky, A. A. Peterson and S. Sun, Active and selective conversion of CO2 to CO on ultrathin Au nanowires, *J Am Chem Soc*, 2014, **136**, 16132–16135.

14 Z. Jin, L. Wang, E. Zuidema, K. Mondal, M. Zhang, J. Zhang, C. Wang, X. Meng, H. Yang and C. Mesters, Hydrophobic zeolite modification for in situ peroxide formation in methane oxidation to methanol, *Science (1979)*, 2020, **367**, 193–197.

15 H. Li, M. Eddaoudi, M. O'Keeffe and O. M. Yaghi, Design and synthesis of an exceptionally stable and highly porous metal-organic framework, *Nature*, 1999, **402**, 276–279.

16 J. Li, H. Huang, W. Xue, K. Sun, X. Song, C. Wu, L. Nie, Y. Li, C. Liu and Y. Pan, Self-adaptive dual-metal-site pairs in metal-organic frameworks for selective CO2 photoreduction to CH4, *Nat Catal*, 2021, **4**, 719–729.

17 C. Wang, W. Fang, Z. Liu, L. Wang, Z. Liao, Y. Yang, H. Li, L. Liu, H. Zhou and X. Qin, Fischer–Tropsch synthesis to olefins boosted by MFI zeolite nanosheets, *Nat Nanotechnol*, 2022, 714-720.

18 W. Dai, X. Wang, G. Wu, N. Guan, M. Hunger and L. Li, Methanol-to-olefin conversion on silicoaluminophosphate catalysts: Effect of Brønsted acid sites and framework structures, *ACS Catal*, 2011, **1**, 292–299.

19 Q. Fu, H. Saltsburg and M. Flytzani-Stephanopoulos, Active nonmetallic Au and Pt species on ceria-based water-gas shift catalysts, *Science (1979)*, 2003, **301**, 935–938.

20 B. Qiao, A. Wang, X. Yang, L. F. Allard, Z. Jiang, Y. Cui, J. Liu, J. Li and T. Zhang, Single-atom catalysis of CO oxidation using Pt1/FeOx, *Nat Chem*, 2011, **3**, 634–641.

21 A. D. Bolatto, M. Wolfire and A. K. Leroy, The CO-to-H2 conversion factor, *Annual Review of Astronomy and Astrophysics*, 2013, **51**, 207-268.

22 S. Dey and N. S. Mehta, Oxidation of carbon monoxide over various nickel oxide catalysts in different conditions: A review, *Chemical Engineering Journal Advances*, 2020, **1**, 100008.

23 F. Jiao, J. Li, X. Pan, J. Xiao, H. Li, H. Ma, M. Wei, Y. Pan, Z. Zhou and M. Li, Selective conversion of syngas to light olefins, *Science (1979)*, 2016, **351**, 1065–1068.

24 K. Cheng, B. Gu, X. Liu, J. Kang, Q. Zhang and Y. Wang, Direct and highly selective conversion of synthesis gas into lower olefins: design of a bifunctional catalyst combining methanol synthesis and carbon–carbon coupling, *Angewandte Chemie*, 2016, **128**, 4803–4806.

25 X. Wu, J. Lang, Z. Sun, F. Jin and Y. H. Hu, Photocatalytic conversion of carbon monoxide: from pollutant removal to fuel production, *Appl Catal B*, 2021, **295**, 120312.

26 D. Glass, R. Quesada-Cabrera, S. Bardey, P. Promdet, R. Sapienza, V. Keller, S. A. Maier, V. Caps, I. P. Parkin and E. Cortés, Probing the Role of Atomic Defects in Photocatalytic Systems through Photoinduced Enhanced Raman Scattering, *ACS Energy Lett*, 2021, **6**, 4273–4281.

27 Y. Zhao, Z. Li, M. Li, J. Liu, X. Liu, G. I. N. Waterhouse, Y. Wang, J. Zhao, W. Gao and Z. Zhang, Reductive transformation of layered-double-hydroxide nanosheets to Fe-based heterostructures for efficient visible-light photocatalytic hydrogenation of CO, *Advanced Materials*, 2018, **30**, 1803127.

28 Z. Li, J. Liu, Y. Zhao, G. I. N. Waterhouse, G. Chen, R. Shi, X. Zhang, X. Liu, Y. Wei and X. Wen, Co-based catalysts derived from layered-double-hydroxide nanosheets for the photothermal production of light Olefins, *Advanced Materials*, 2018, **30**, 1800527.

29 Y. Zhao, B. Zhao, J. Liu, G. Chen, R. Gao, S. Yao, M. Li, Q. Zhang, L. Gu and J. Xie, Oxide-modified nickel photocatalysts for the production of hydrocarbons in visible light, *Angewandte Chemie*, 2016, **128**, 4287–4291.

30 Z. Li, X. Zhang, J. Liu, R. Shi, G. I. N. Waterhouse, X. Wen and T. Zhang, Titania-Supported Ni2P/Ni Catalysts for Selective Solar-Driven CO Hydrogenation, *Advanced Materials*, 2021, **33**, 2103248.

31 R. Mu, A. Dahal, Z.-T. Wang, Z. Dohnálek, G. A. Kimmel, N. G. Petrik and I. Lyubinetsky, Adsorption and photodesorption of CO from charged point defects on TiO2 (110), *J Phys Chem Lett*, 2017, **8**, 4565–4572.

32 A. V Vutolkina, I. G. Baygildin, A. P. Glotov, K. A. Cherednichenko, A. L. Maksimov and E. A. Karakhanov, Dispersed Ni-Mo sulfide catalysts from water-soluble precursors for HDS of BT and DBT via in situ produced H2 under Water gas shift conditions, *Appl Catal B*, 2021, **282**, 119616.

33 A. V Vutolkina, A. P. Glotov, A. V Zanina, D. F. Makhmutov, A. L. Maximov, S. V Egazar'yants and E. A. Karakhanov, Mesoporous Al-HMS and Al-MCM-41 supported Ni-Mo sulfide catalysts for HYD and HDS via in situ hydrogen generation through a WGSR, *Catal Today*, 2019, **329**, 156–166.

34 A. V Vutolkina, I. G. Baygildin, A. P. Glotov, K. A. Cherednichenko, A. L. Maksimov and E. A. Karakhanov, Dispersed Ni-Mo sulfide catalysts from water-soluble precursors for HDS of BT and DBT via in situ produced H2 under Water gas shift conditions, *Appl Catal B*, 2021, **282**, 119616.

35 L. Yao, Y. Pan, X. Shen, D. Wu, A. Bentalib and Z. Peng, Utilizing hydrogen underpotential deposition in CO reduction for highly selective formaldehyde production under ambient conditions, *Green Chemistry*, 2020, **22**, 5639–5647.

36 S. Dey and N. S. Mehta, Oxidation of carbon monoxide over various nickel oxide catalysts in different conditions: A review, *Chemical Engineering Journal Advances*, 2020, **1**, 100008.

37 S. Dey, G. C. Dhal, D. Mohan and R. Prasad, Low-temperature complete oxidation of CO over various manganese oxide catalysts, *Atmos Pollut Res*, 2018, **9**, 755–763.

38 S. Dey and G. C. Dhal, The catalytic activity of cobalt nanoparticles for low-temperature oxidation of carbon monoxide, *Mater Today Chem*, 2019, **14**, 100198.

39 X. Zhang, H. Li, F. Hou, Y. Yang, H. Dong, N. Liu, Y. Wang and L. Cui, Synthesis of highly efficient Mn2O3 catalysts for CO oxidation derived from Mn-MIL-100, *Appl Surf Sci*, 2017, **411**, 27–33.

40 P. Schlexer, D. Widmann, R. J. Behm and G. Pacchioni, CO oxidation on a Au/TiO2 nanoparticle catalyst via the Au-assisted Mars–van Krevelen mechanism, *ACS Catal*, 2018, **8**, 6513–6525.

41 Y. Pan, X. Shen, M. A. Holly, L. Yao, D. Wu, A. Bentalib, J. Yang, J. Zeng and Z. Peng, Oscillation of Work Function during Reducible Metal Oxide Catalysis and Correlation with the Activity Property, *ChemCatChem*, 2020, **12**, 85–89.

42 V. M. Shinde and G. Madras, Synthesis of nanosized Ce0. 85M0. 1Ru0. 05O2− δ (M= Si, Fe) solid solution exhibiting high CO oxidation and water gas shift activity, *Appl Catal B*, 2013, **138**, 51–61.

43 G. Cao, N. A. Deskins and N. Yi, Carbon monoxide oxidation over copper and nitrogen modified titanium dioxide⋆, *Appl Catal B*, 2021, **285**, 119748.

44 W. Chen, Y. Ma, F. Li, L. Pan, W. Gao, Q. Xiang, W. Shang, C. Song, P. Tao and H. Zhu, Strong Electronic Interaction of Amorphous Fe2O3 Nanosheets with Single-Atom Pt toward Enhanced Carbon Monoxide Oxidation, *Adv Funct Mater*, 2019, **29**, 1904278.

45 S. Dey, G. C. Dhal, D. Mohan and R. Prasad, Kinetics of catalytic oxidation of carbon monoxide over CuMnAgOx catalyst, *Materials discovery*, 2017, **8**, 18–25.

46 S. Dey and N. S. Mehta, To optimized various parameters of Hopcalite catalysts in the synthetic processes for low temperature CO oxidation, *Applications in Energy and Combustion Science*, 2021, **6**, 100031.

47 Y. Zhu, X. Pan, F. Jiao, J. Li, J. Yang, M. Ding, Y. Han, Z. Liu and X. Bao, Role of manganese oxide in syngas conversion to light olefins, *ACS Catal*, 2017, **7**, 2800–2804.

48 V. Masson-Delmotte, P. Zhai, H.-O. Pörtner, D. C. Roberts, J. Skea, P. R. Shukla, A. Pirani, W. Moufouma-Okia, C. Péan and R. Pidcock, *Global warming of 1.5° C: Summary for policy makers,* IPCC - The Intergovernmental Panel on Climate Change, Geneva, 2018.

49 S. Zhang, Q. Fan, R. Xia and T. J. Meyer, CO2 reduction: from homogeneous to heterogeneous electrocatalysis, *Acc Chem Res*, 2020, **53**, 255–264.

50 M. González-Castaño, B. Dorneanu and H. Arellano-García, The reverse water gas shift reaction: a process systems engineering perspective, *React Chem Eng*, 2021, **6**, 954–976.

51 W. J. Lee, C. Li, H. Prajitno, J. Yoo, J. Patel, Y. Yang and S. Lim, Recent trend in thermal catalytic low temperature CO2 methanation: A critical review, *Catal Today*, 2021, **368**, 2–19.

52 M. Marchese, G. Buffo, M. Santarelli and A. Lanzini, CO2 from direct air capture as carbon feedstock for Fischer-Tropsch chemicals and fuels: Energy and economic analysis, *Journal of CO2 Utilization*, 2021, **46**, 101487.

53 H. S. Lim, M. Lee, Y. Kim, D. Kang and J. W. Lee, Low-temperature CO2 hydrogenation to CO on Ni-incorporated LaCoO3 perovskite catalysts, *Int J Hydrogen Energy*, 2021, **46**, 15497–15506.

54 Y. Ma, Z. Guo, Q. Jiang, K.-H. Wu, H. Gong and Y. Liu, Molybdenum carbide clusters for thermal conversion of CO2 to CO via reverse water-gas shift reaction, *Journal of Energy Chemistry*, 2020, **50**, 37–43.

55 J. Zhu, P. Wang, X. Zhang, G. Zhang, R. Li, W. Li, T. P. Senftle, W. Liu, J. Wang and Y. Wang, Dynamic structural evolution of iron catalysts involving competitive oxidation and carburization during CO2 hydrogenation, *Sci Adv*, 2022, **8**, eabm3629.

56 Z. Ma and M. D. Porosoff, Development of tandem catalysts for CO2 hydrogenation to olefins, *ACS Catal*, 2019, **9**, 2639–2656.

57 M. Behrens, F. Studt, I. Kasatkin, S. Kühl, M. Hävecker, F. Abild-Pedersen, S. Zander, F. Girgsdies, P. Kurr and B.-L. Kniep, The active site of methanol synthesis over Cu/ZnO/Al2O3 industrial catalysts, *Science (1979)*, 2012, **336**, 893–897.

58 O. Martin, A. J. Martín, C. Mondelli, S. Mitchell, T. F. Segawa, R. Hauert, C. Drouilly, D. Curulla-Ferré and J. Pérez-Ramírez, Indium oxide as a superior catalyst for methanol synthesis by CO2 hydrogenation, *Angewandte Chemie International Edition*, 2016, **55**, 6261–6265.

59 J. Wang, G. Li, Z. Li, C. Tang, Z. Feng, H. An, H. Liu, T. Liu and C. Li, A highly selective and stable ZnO-ZrO2 solid solution catalyst for CO2 hydrogenation to methanol, *Sci Adv*, 2017, **3**, e1701290.

60 M. S. Frei, C. Mondelli, A. Cesarini, F. Krumeich, R. Hauert, J. A. Stewart, D. Curulla Ferré and J. Pérez-Ramírez, Role of zirconia in indium oxide-catalyzed CO2 hydrogenation to methanol, *ACS Catal*, 2019, **10**, 1133–1145.

61 L. Yao, X. Shen, Y. Pan and Z. Peng, Synergy between active sites of Cu-In-Zr-O catalyst in CO2 hydrogenation to methanol, *J Catal*, 2019, **372**, 74–85.

62 M. S. Frei, C. Mondelli, R. García-Muelas, K. S. Kley, B. Puértolas, N. López, O. v Safonova, J. A. Stewart, D. Curulla Ferré and J. Pérez-Ramírez, Atomic-scale engineering of indium oxide promotion by palladium for methanol production via CO2 hydrogenation, *Nat Commun*, 2019, **10**, 3377.

63 T. Pinheiro Araújo, C. Mondelli, M. Agrachev, T. Zou, P. O. Willi, K. M. Engel, R. N. Grass, W. J. Stark, O. V Safonova and G. Jeschke, Flame-made ternary Pd-In2O3-ZrO2 catalyst with enhanced oxygen vacancy generation for CO2 hydrogenation to methanol, *Nat Commun*, 2022, **13**, 5610.

64 L. Yao, Y. Pan, D. Wu, J. Li, R. Xie and Z. Peng, Approaching full-range selectivity control in CO 2 hydrogenation to methanol and carbon monoxide with catalyst composition regulation, *Inorg Chem Front*, 2021, **8**, 2433–2441.

65 L. Yao, X. Shen, Y. Pan and Z. Peng, Unravelling proximity-driven synergetic effect within CIZO–SAPO bifunctional catalyst for CO2 hydrogenation to DME, *Energy & Fuels*, 2020, **34**, 8635–8643.

66 S. Gao, Y. Lin, X. Jiao, Y. Sun, Q. Luo, W. Zhang, D. Li, J. Yang and Y. Xie, Partially oxidized atomic cobalt layers for carbon dioxide electroreduction to liquid fuel, *Nature*, 2016, **529**, 68–71.

67 T. Baran, S. Wojtyła, A. Dibenedetto, M. Aresta and W. Macyk, Zinc sulfide functionalized with ruthenium nanoparticles for photocatalytic reduction of CO2, *Appl Catal B*, 2015, **178**, 170–176.

68 W. Tu, Y. Li, L. Kuai, Y. Zhou, Q. Xu, H. Li, X. Wang, M. Xiao and Z. Zou, Construction of unique two-dimensional MoS 2–TiO 2 hybrid nanojunctions: MoS 2 as a promising cost-effective cocatalyst toward improved photocatalytic reduction of CO 2 to methanol, *Nanoscale*, 2017, **9**, 9065–9070.

69 J. Wang, S. Lin, N. Tian, T. Ma, Y. Zhang and H. Huang, Nanostructured metal sulfides: classification, modification strategy, and solar-driven CO2 reduction application, *Adv Funct Mater*, 2021, **31**, 2008008.

70 X. Meng, X. Cui, N. P. Rajan, L. Yu, D. Deng and X. Bao, Direct methane conversion under mild condition by thermo-, electro-, or photocatalysis, *Chem*, 2019, **5**, 2296–2325.

71 E. McFarland, Unconventional chemistry for unconventional natural gas, *Science (1979)*, 2012, **338**, 340–342.

72 E. Tabor, J. Dedecek, K. Mlekodaj, Z. Sobalik, P. C. Andrikopoulos and S. Sklenak, Dioxygen dissociation over man-made system at room temperature to form the active α-oxygen for methane oxidation, *Sci Adv*, 2020, **6**, eaaz9776.

73 Y. Xing, Z. Yao, W. Li, W. Wu, X. Lu, J. Tian, Z. Li, H. Hu and M. Wu, Fe/Fe3C boosts H2O2 utilization for methane conversion overwhelming O2 generation, *Angewandte Chemie*, 2021, **133**, 8971–8977.

74 P. Wang, G. Zhao, Y. Wang and Y. Lu, MnTiO3-driven low-temperature oxidative coupling of methane over TiO2-doped Mn2O3-Na2WO4/SiO2 catalyst, *Sci Adv*, 2017, **3**, e1603180.

75 Z. Liang, T. Li, M. Kim, A. Asthagiri and J. F. Weaver, Low-temperature activation of methane on the IrO2 (110) surface, *Science (1979)*, 2017, **356**, 299–303.

76 N. Xu, C. A. Coco, Y. Wang, T. Su, Y. Wang, L. Peng, Y. Zhang, Y. Liu, J. Qiao and X.-D. Zhou, Electro-conversion of methane to alcohols on “capsule-like” binary metal oxide catalysts, *Appl Catal B*, 2021, **282**, 119572.

77 H. Stotz, L. Maier, A. Boubnov, A. T. Gremminger, J.-D. Grunwaldt and O. Deutschmann, Surface reaction kinetics of methane oxidation over PdO, *J Catal*, 2019, **370**, 152–175.

78 Z.-Q. Wang, D. Wang and X.-Q. Gong, Strategies to improve the activity while maintaining the selectivity of oxidative coupling of methane at La2O3: a density functional theory study, *ACS Catal*, 2019, **10**, 586–594.

79 Z. Liu, E. Huang, I. Orozco, W. Liao, R. M. Palomino, N. Rui, T. Duchoň, S. Nemšák, D. C. Grinter and M. Mahapatra, Water-promoted interfacial pathways in methane oxidation to methanol on a CeO2-Cu2O catalyst, *Science (1979)*, 2020, **368**, 513–517.

80 J. Gao, Y. Zheng, J.-M. Jehng, Y. Tang, I. E. Wachs and S. G. Podkolzin, Identification of molybdenum oxide nanostructures on zeolites for natural gas conversion, *Science (1979)*, 2015, **348**, 686–690.

81 S. Park, J. M. Vohs and R. J. Gorte, Direct oxidation of hydrocarbons in a solid-oxide fuel cell, *Nature*, 2000, **404**, 265–267.

82 L. Fan, C. Li, P. V. Aravind, W. Cai, M. Han and N. Brandon, Methane reforming in solid oxide fuel cells: Challenges and strategies, *J Power Sources*, 2022, **538**, 231573.

83 M. E. O’Reilly, R. S. Kim, S. Oh and Y. Surendranath, Catalytic methane monofunctionalization by an electrogenerated high-valent Pd intermediate, *ACS Cent Sci*, 2017, **3**, 1174–1179.

84 R. S. Kim and Y. Surendranath, Electrochemical Reoxidation

Enables Continuous Methane-to-Methanol Catalysis with Aqueous Pt Salts, *ACS Cent Sci*, 2019, **5**, 1179–1186.

85 B. Lee and T. Hibino, Efficient and selective formation of methanol from methane in a fuel cell-type reactor, *J Catal*, 2011, **279**, 233–240.

86 J. Deng, S.-C. Lin, J. Fuller, J. A. Iñiguez, D. Xiang, D. Yang, G. Chan, H. M. Chen, A. N. Alexandrova and C. Liu, Ambient methane functionalization initiated by electrochemical oxidation of a vanadium (V)-oxo dimer, *Nat Commun*, 2020, **11**, 3686.

87 J. Li, L. Yao, D. Wu, J. King, S. S. C. Chuang, B. Liu and Z. Peng, Electrocatalytic Methane Oxidation to Ethanol on Iron-Nickel Hydroxide Nanosheets, *Appl Catal B*, 2022, 121657.

88 N. Spinner and W. E. Mustain, Electrochemical methane activation and conversion to oxygenates at room temperature, *ECS Trans*, 2013, **53**, 1.

89 Y. Song, Y. Zhao, G. Nan, W. Chen, Z. Guo, S. Li, Z. Tang, W. Wei and Y. Sun, Electrocatalytic oxidation of methane to ethanol via NiO/Ni interface, *Appl Catal B*, 2020, **270**, 118888.

90 M. Ma, B. J. Jin, P. Li, M. S. Jung, J. Il Kim, Y. Cho, S. Kim, J. H. Moon and J. H. Park, Ultrahigh electrocatalytic conversion of methane at room temperature, *Advanced Science*, 2017, **4**, 1700379.

91 M. Ma, C. Oh, J. Kim, J. H. Moon and J. H. Park, Electrochemical CH4 oxidation into acids and ketones on ZrO2: NiCo2O4 quasi-solid solution nanowire catalyst, *Appl Catal B*, 2019, **259**, 118095.

92 R. A. Van Santen, M. Neurock and S. G. Shetty, Reactivity theory of transition-metal surfaces: a Brønsted− Evans− Polanyi linear activation energy− free-energy analysis, *Chem Rev*, 2009, **110**, 2005–2048.

93 S. Trasatti, Electrocatalysis by oxides—attempt at a unifying approach, *J Electroanal Chem Interfacial Electrochem*, 1980, **111**, 125–131.

94 G. Kumar, S. L. J. Lau, M. D. Krcha and M. J. Janik, Correlation of methane activation and oxide catalyst reducibility and its implications for oxidative coupling, *ACS Catal*, 2016, **6**, 1812–1821.

95 J. Suntivich, K. J. May, H. A. Gasteiger, J. B. Goodenough and Y. Shao-Horn, A perovskite oxide optimized for oxygen evolution catalysis from molecular orbital principles, *Science (1979)*, 2011, **334**, 1383–1385.

96 J. K. Nørskov, T. Bligaard, J. Rossmeisl and C. H. Christensen, Towards the computational design of solid catalysts, *Nat Chem*, 2009, **1**, 37–46.

97 J. Li, X. Shen, Y. Pan and Z. Peng, Fingerprinting the Ammonia Synthesis Pathway Using Spatiotemporal Electrostatic Potential Distribution of Intermediates, *ACS Omega*, 2021, **6**, 6292–6296.

98 P. Schwach, X. Pan and X. Bao, Direct conversion of methane to value-added chemicals over heterogeneous catalysts: challenges and prospects, *Chem Rev*, 2017, **117**, 8497–8520.